2024, 21(4): 1243-1254
https://doi.org/10.21123/bsj.2023.8458
P-ISSN: 2078-8665 - E-ISSN: 2411-7986
Baghdad Science Journal

Conducting Polyanethole /Metals Oxides Nanocomposites for Corrosion Protection and Bioactivity

Ayat Monther Alqudsi *, Khulood Abid Saleh

Department of Chemistry, College of Science, University of Baghdad, Baghdad, Iraq.
*Corresponding Author.

Received 15/01/2023, Revised 27/03/2023, Accepted 29/03/2023, Published Online First 20/09/2023, Published 01/04/2024

Abstract

Corrosion is critical to a researcher since it has a substantial impact on both people's safety and the economy. A new approach based on a unique material has been employed to prevent rusting. Conducting polymer-composites are material types that show promise for anticorrosion by electrochemical synthesis of polyanethole(PA)/metals oxide nanocomposite (ZnO,TiO_2) on Stainless Steel 304L (SS-304L) which plays as working electrode by using electropolymerization technique. The synthesized coating polymer was characterized by Fourier transform-infrared spectroscopy (FTIR) and atomic force microscopy (AFM) checkups. The findings demonstrated that when compared to the blank SS- 304L, PA/Nano composite and PA provide the strongest corrosion defenses for the metal. The results explained that the corrosion protection increased from 71% for PA film to 98% for PA/ZnO film and to 87% for PA/TiO_2 at 298K .In addition, calculations were made for the kinetic and thermodynamic parameters (Ea, A, ΔH, ΔS and ΔG). Escherichia coli and Staphylococcus aureus, two gram-positive and gram-negative bacteria, were used to test the biological activity of polymeric film (E.Coli).

Keywords: Anethole, Corrosion, Electropolymerization, Nanocomposite, Polyanethole.

Introduction

Process of electrochemical polymerization includes the monomer being oxidized to create radical, then the radical cations interacted with one other or with another monomer to form a radical dimer, which subsequently moved to a trimer with a longer chain length[1]. Electro polymerization has been described for monomers such as methyl methacrylate[2], styrene[3], aniline as a poly methyl aniline[4], and pyrrole[5]. The electrochemical polymerization process required a precise interaction between the working electrode and the monomer, resulting in strong coating adherence[6].

In anise oil, Anethole (1-Methoxy-4-[(1E)-prop-1-en-1-yl]benzene) plays a significant role. The oil is a colorless to pale-yellow liquid or crystalline mass with a powerful, sweet odor which is characteristic of anethole, its chemical structure explained in Scheme 1, and this oil is used for flavoring foods, beverages, and oral hygiene products[7]. Anethole is a naturally occurring aromatic oxidant found in a wide range of medicinal plant extracts and is widely employed in the food and beverage industries[8]. Several studies in recent years have revealed that anethole has numerous beneficial effects for human

2024, 21(4): 1243-1254
https://doi.org/10.21123/bsj.2023.8458
P-ISSN: 2078-8665 - E-ISSN: 2411-7986
Baghdad Science Journal

health, including anti-inflammatory, anticarcinogenic and chemopreventive, antidiabetic, immunomodulatory, neuroprotective, and antithrombotic effects that are mediated by the modulation of several cell signaling pathways[9,10].

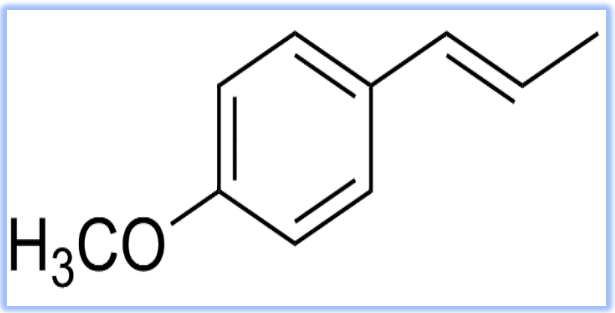

Scheme 1. Molecular structure of Anethole.

P. Cerrai and colleagues investigated the electrochemical behavior of the system using voltammetry at rotating and stationary Pt electrodes as well as chronoamperometry to study the cationic electropolymerization of trans-anethole initiated by a direct electron transfer mechanism at a Pt anode in a 1,2-dichloroethane solution[11]. Maksim I. Hulnik studied the quasiliving cationic polymerization of the naturally occurring β-methylstyrene derivative, anethole, was reported for the first time and the effect of solvent polarity, initiator nature as well as Lewis acid, proton trap, and initiator concentrations on the cationic polymerization of anethole in the presence of $SnCl_4$ as a coinitiator was studied in detail[12].

Nano polymer composite coating and conducting polymer coating are currently widely used in a number of applications. Studies on conducting polymers, nanopolymer composite coatings, and their combinations have advanced significantly. In addition to great efficiency and clever corrosion defenses, several unique nontoxic corrosion protection compounds have also improved long periods of efficacy and simplicity of manufacture. Coatings with long-term corrosion resistance, strong adhesions, improved durability, and outstanding surface mechanical abrasion resistance were in high demand. It has been demonstrated that using nano particles in polymer coatings can improve not only the barrier effects but also the electrochemical anticorrosion and other performance characteristics such as adhesions, thermal stabilities, mechanical strengths, magnetonstatic shielding, and hydrophobic properties[12,13]. Many different kinds of oxides nano particles, such as TiO_2, ZnO, Al_2O_3, CeO_2, SiO_2 and Nano clays, were applied to polymer coating and shown superior protective properties than standard polymer coating[14-16].

In this study, conducting polymer films were generated on SS-304L by electrochemical polymerization process, and polymer nanocomposites containing ZnO and TiO_2 were evaluated for corrosion protection in 3.5% NaCl solution at temperatures range (298-328) K.

Materials and Methods

Chemicals

Stainless Steel alloys (SS-304 L) specimens of 2 ×2 cm^2 area with chemical composition as described in the Table 1 were obtained from commercially SS-304L sheet of 0.5mm thickness

Table 1. Chemical composition for SS-304L.

material	*C*	*Mn*	*Si*	*S*	*P*	*Cr*	*Ni*	*Fe*
SS 304 L	0.019	1.53	0.50	0.030	0.030	18.20	8.04	balance

These samples were polished using emery sheets of various grades [600, 800, 1200, and 2000] mesh grit, and then washed with tap water, distilled water, ethanol, and finally acetone before being dried with a hot air drier. The materials used are listed in the Table 2, below

2024, 21(4): 1243-1254
https://doi.org/10.21123/bsj.2023.8458
P-ISSN: 2078-8665 - E-ISSN: 2411-7986
Baghdad Science Journal

Table 2. The Chemical materials were used.

Raw Material	*Molecular Formula*	*Supplier*	*Purity*
Anethole	$C_{10}H_{12}O$	Sigma-Aldrich	99%
Ethanol	C_2H_5OH	GCC	99.9%
Oxalic acid	$H_2C_2O_4$	BDH	99%
Sodium Chloride	NaCl	BDH	99.5%
Sulpharic acid	H_2SO_4	GCC	98%
Sodium hydroxide	NaOH	BDH	99%
Zinc Oxide	ZnO	Hongwe nanometer	99%
Titanium oxide	TiO_2	Hongwe nanometer	99%
Di - Methyl Sulfoxide	$(CH_3)_2SO$	LOBA Chemie	98%

Cyclic voltammetry and Electro-Polymerization of the Anethole Monomer: Cyclic Voltammetry is used to determine the electropolymerization potential. A solution of 10mM Anethole in 70% 0.1M NaOH was prepared, and three drops of concentrated H_2SO_4 were added to improve electrolyte conductivity within a potential range of (-2000 to 2000) mV vs. standard calomel electrode. Fig. 1, shows the consecutive cyclic voltammogram made using PA at around 0.85 volts.

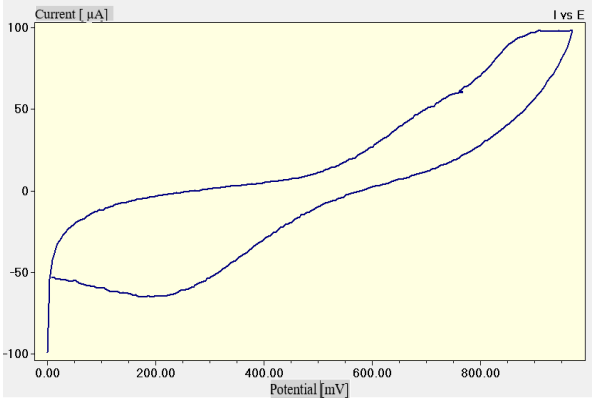

Figure 1. The cyclic voltammogram of PA.

The Electropolymerization of Anethole: The SS-304L working electrodes (anode) were immersed in 0.1 M NaOH containing 10 mM Anethole with three drops of H_2SO_4 (99%) and 0.1 g of oxalic acid as a supporting electrolyte, and a long rod of graphene was used as the counter electrode (cathode). At room temperature, a voltage of 0.85 V was applied for 60 minutes.

Electrochemical Polymerization of the Anethole with metals oxides nanoparticles: After dispersion, 0.02 g more of n-ZnO was added to the monomer solution, also with 0.02 g of n-TiO_2 to strengthen the coating layer against corrosion and biological activity as shown in Scheme 2.

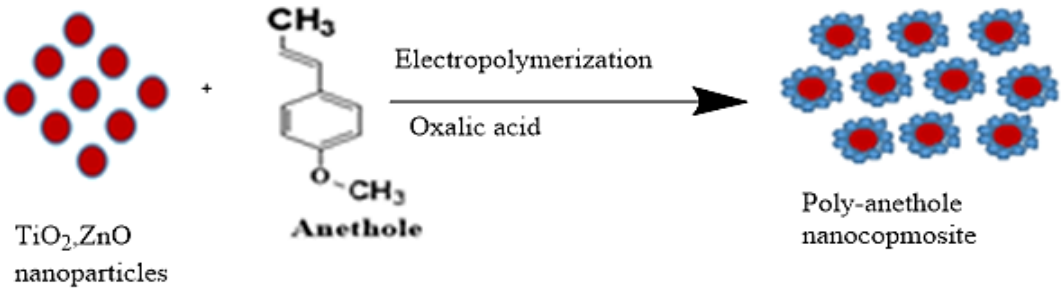

Scheme 2. Electropolymerization of the Anethole with nano-oxides to polymer composite.

Electro Chemical Corrosion Study: Three electrodes have been used as a cell in a corrosion study: a working electrode (SS-304L, coated and uncoated), a reference electrode (SCE), and a counter

2024, 21(4): 1243-1254
https://doi.org/10.21123/bsj.2023.8458
P-ISSN: 2078-8665 - E-ISSN: 2411-7986
Baghdad Science Journal

or auxiliary electrode (platinum electrode). Under potentiostatic circumstances, coated and uncoated SS-304L were subjected to anodic and cathodic polarization for the corrosion of SS-304L at temperatures between 293 and 323 K.

Results and Discussion

FTIR Spectroscopy of the *(PA)*: The PA and Anethole monomer have been produced on an SS 304L alloy by electrochemical polymerization were studied using FTIR spectra, which are shown in Fig. 2. The peak C=C in the hydrocarbon chain of Anethole (in alkenes in general) is attributed to the absorption bands at 1680 cm^{-1} in Fig. 2, although the PA IR spectra do not show this peak. The peak at around 3299 cm^{-1}, which is not present in the IR spectra of Anethole, may be ascribed to intramolecular H-bonds between the repeating units of PA chains[15].

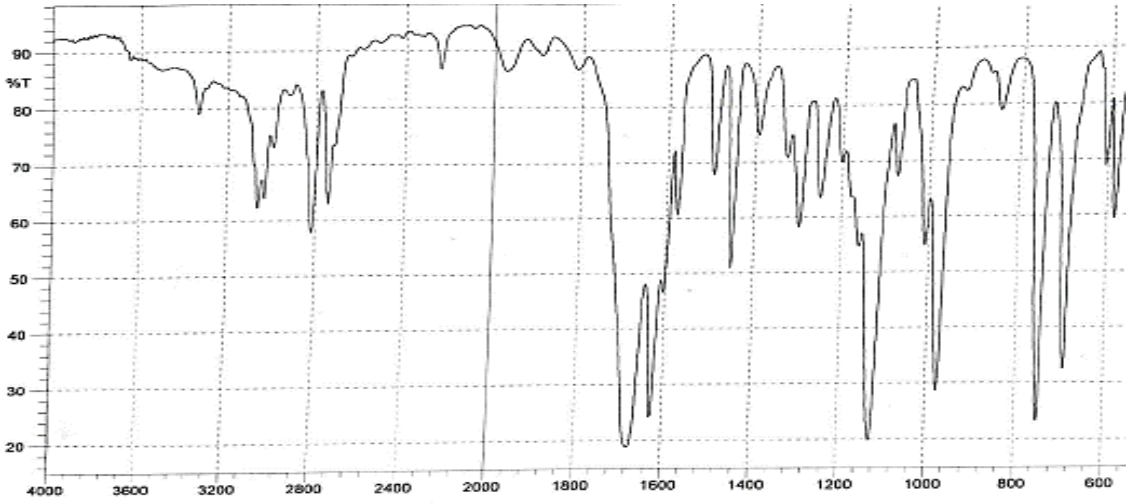

a

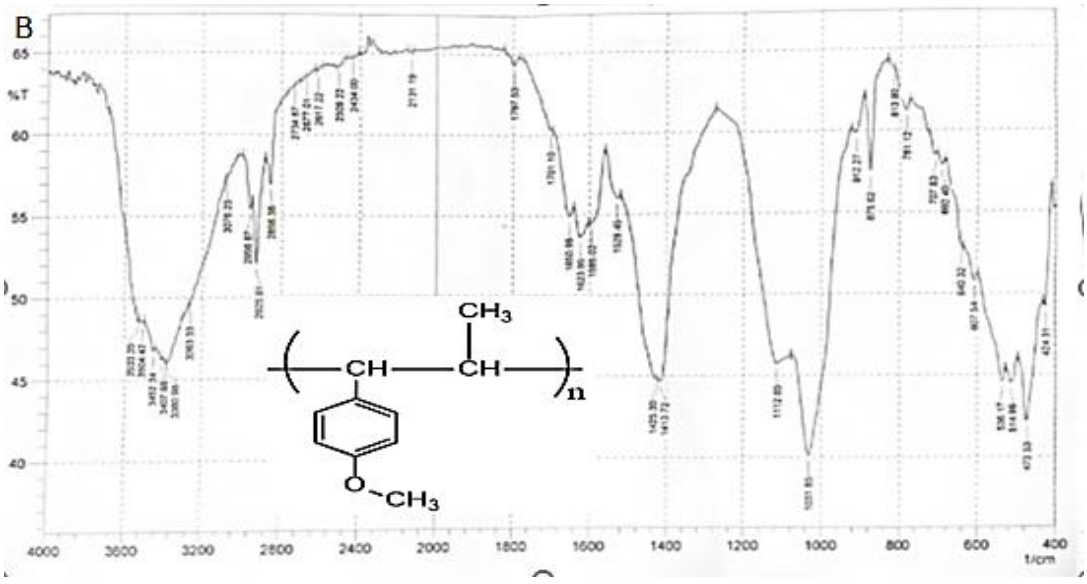

b

Figure 2. FTIR for a. Anethole, b. Polyanethole.

2024, 21(4): 1243-1254
https://doi.org/10.21123/bsj.2023.8458
P-ISSN: 2078-8665 - E-ISSN: 2411-7986
Baghdad Science Journal

AFM for PA and the both nano-PA: The surface topography of SS-304L coated with PA was examined using the AFM Technique in the presence as well as absence of nanoparticles (TiO_2 and ZnO). Fig. 3, displays 2D and 3D AFM images of every coating film that has been used. The most popular metrics for assessing the roughness of a surface using AFM-analysis are **RMS:** the mean grain size, root mean square, and **Ra:** roughness average. According to the findings, as shown in Table 3. The use of nanoparticles to reduce the grain size of PA resulted in a reduction in surface roughness for all coated films. Therefore, the less rough the surface, the greater the barrier effect for avoiding coating corrosion[16,17].

Table 3. AFM parameters to coated SS-304L with PA both when present and when absent of the nanomaterials.

Samples	(Ra) (nm)	(Rq)(nm)	mean grainsize(nm)
coated of polymer **PA**	7.391	8.547	199.1
coated of polymer **PA modified by ZnO**	1.175	1.259	190.9
coated of polymer **PA modified by TiO_2**	2.560	2.903	167.9

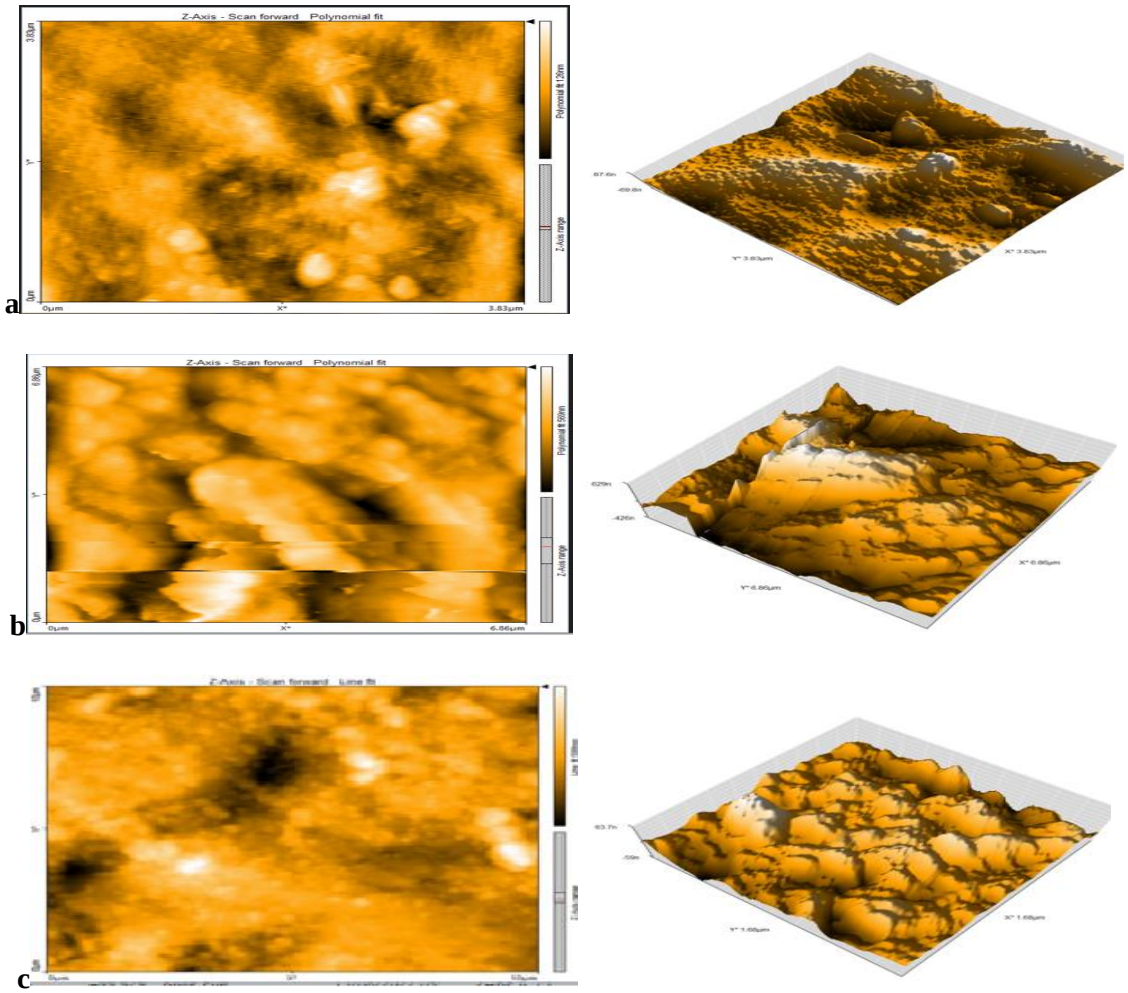

Figure 3. The AFM Images to: a- PA, b-PA with n-ZnO , c-PA with n-TiO_2.

Corrosion Measurements: The influence of a polymeric layer on the cathodic and anodic polarization curves of SS-304L in a 3.5% of NaCl solution at temperatures range 298 - 328 K in the presence and absence of the nano metal

2024, 21(4): 1243-1254
https://doi.org/10.21123/bsj.2023.8458
P-ISSN: 2078-8665 - E-ISSN: 2411-7986
Baghdad Science Journal

oxides shown in Fig. 4 the extrapolation of Tafel curves to calculate the corrosion current density. The impact of the polymeric layer on the presence and absence of the nanomaterials is shown in Table 4. The corrosion parameters were weight loss (WL), penetration loss (PL), cathodic Tafel slope (bc), anodic Tafel slope (ba), corrosion potential ($E_{COR.}$), and corrosion current density ($I_{COR.}$). The following equation was used to compute protection effectiveness (PE%)[17]

Protection efficiency **(PE%)=[$(I_{COR.})_{uncoated}$-$(I_{COR.})_{coated}$]/$(I_{COR.})_{uncoated}$……2**

where, $(I_{COR.})_{uncoated}$:the corrosion current density for uncoated SS 304L (blank),

$(I_{COR.})_{coated}$: current density of coated SS-304L for corrosion

In the meanwhile, the polarization resistance of corrosion (Rp) was computed using this equation (the Stern-Geary equation)[18]

Rp=(βa+βc)/2.303(βaβc)*$I_{COR.}$……3

The results showed that when the temperature increases, both ($E_{COR.}$) and ($I_{COR.}$) increased. By increasing temperatures, the corrosion potential ($E_{COR.}$) moved to more active values (cathodic). After adding nanomaterial (ZnO,TiO_2), the corrosion current density for coated SS-304L significantly reduced as compared to uncoated SS-304L. Inferring that the corrosion protection also serves as anodic protection, it was found from Tafel plots that $E_{COR.}$ For the coated SS-304L changed into a higher position (noble direction) than the $E_{COR.}$ For blank SS-304L. Additionally, the Rp values are higher than those of uncoated SS 304L, particularly after the addition of nanomaterials[19,20].

Table 4. Corrosion parameters for uncoated and coated SS-304L in 3.5% NaCl at a temperature range (298-328) K.

Samples	T(K)	-$E_{COR.}$ (mV)	$I_{COR.}$ (μA/cm^2)	-βc (mV/Dec	βa (mV Dec)	WL (gm/m^2.d)	Rp (Ω/cm^2))	PL (mm/y)	PE%
Uncoated	298	376	8.78	124.2	130.5	2.2	3147.13	$9.79*10^{-2}$	-
	308	374	21.47	160.8	155.0	5.38	1596.17	$2.40*10^{-1}$	-
	318	394	36.95	177.2	170.4	10.3	1020.81	$4.57*10^{-1}$	-
	328	405	49.57	192.1	190.4	15.4	837.62	$6.87*10^{-1}$	-
Coated	298	89	2.53	90.8	83.1	1.39	7446.85	$6.17*10^{-2}$	71
PA	308	109	7.11	94.1	83.2	1.78	2696.74	$7.94*10^{-2}$	66
	318	120	13.11	96.1	78.9	3.79	1435.04	$1.69*10^{-1}$	64
	328	131	18.35	91.6	80.4	4.6	1013.19	$2.05*10^{-1}$	62
Coated	298	183	$187.3*10^{-3}$	59.2	70.4	$4.69*10^{-2}$	74671.3	$2.09*10^{-3}$	98
PA+ZnO	308	204	$541.5*10^{-3}$	81.8	70.5	$1.36*10^{-1}$	30391.4	$6.04*10^{-3}$	97
	318	217	2.15	86.3	90.2	$5.38*10^{-1}$	8907.17	$2.39*10^{-2}$	94
	328	239	3.76	87.3	79.4	$9.43*10^{-1}$	4801.94	$4.2*10^{-2}$	92
Coated	298	200	1.13	46.4	48.4	$2.59*10^{-1}$	9102.95	$1.15*10^{-2}$	87
PA+TiO_2	308	201	3.04	68.5	53	$5.88*10^{-1}$	4267.98	$2.62*10^{-2}$	85
	318	220	6.01	57.4	56.3	$7.53*10^{-1}$	2053.48	$3.35*10^{-2}$	83
	328	234	8.98	73.4	70.9	1.52	1743.83	$6.79*10^{-2}$	81

2024, 21(4): 1243-1254
https://doi.org/10.21123/bsj.2023.8458
P-ISSN: 2078-8665 - E-ISSN: 2411-7986
Baghdad Science Journal

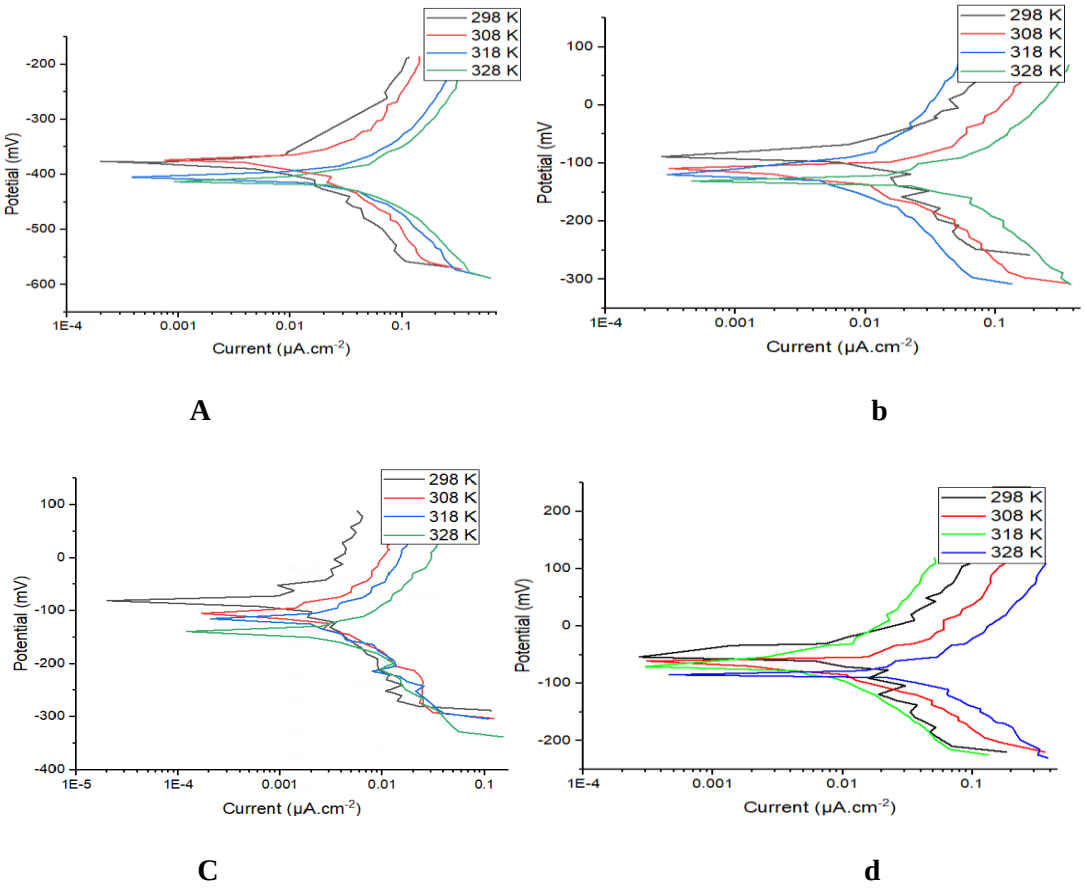

Figure 4. Tafel plots for SS-304L a) uncoated, b) coated by PA, c) coated by PA modified with ZnO ,d) coated by PA modified with TiO_2.

Kinetic and Thermodynamic of Corrosion

The impact of temperature on the corrosion rate of uncoated and coated SS-304L in 3.5% NaCl solution has been investigated using a similar Arrhenius equation for the temperature range 298-328 K[21].

$Ic_{OR.}=Ae^{-Ea/RT}$…..3 which converted to logarithm form

Where Ic_{OR} and A are the current density of corrosion and Arrhenius factor respectively. Ea (J moL^{-1}) is the Activation energy, T (K) is the temperature, and R shows the global constant (J moL^{-1} K^{-1})

Log $Ic_{OR.}$=Log A-(Ea / 2.303RT)……4

The transition state equation is shown below:[22]

log ($Ic_{OR.}$/ T) = [log (R / Nh)] + [ΔS / 2.303 R]– [ΔH / 2.303 RT]……*5*

The activation of free energy was decided from Eq. 5 below:

$$\Delta G^* = \Delta H^* - T\Delta S^* \ldots.6$$

2024, 21(4): 1243-1254
https://doi.org/10.21123/bsj.2023.8458
P-ISSN: 2078-8665 - E-ISSN: 2411-7986
Baghdad Science Journal

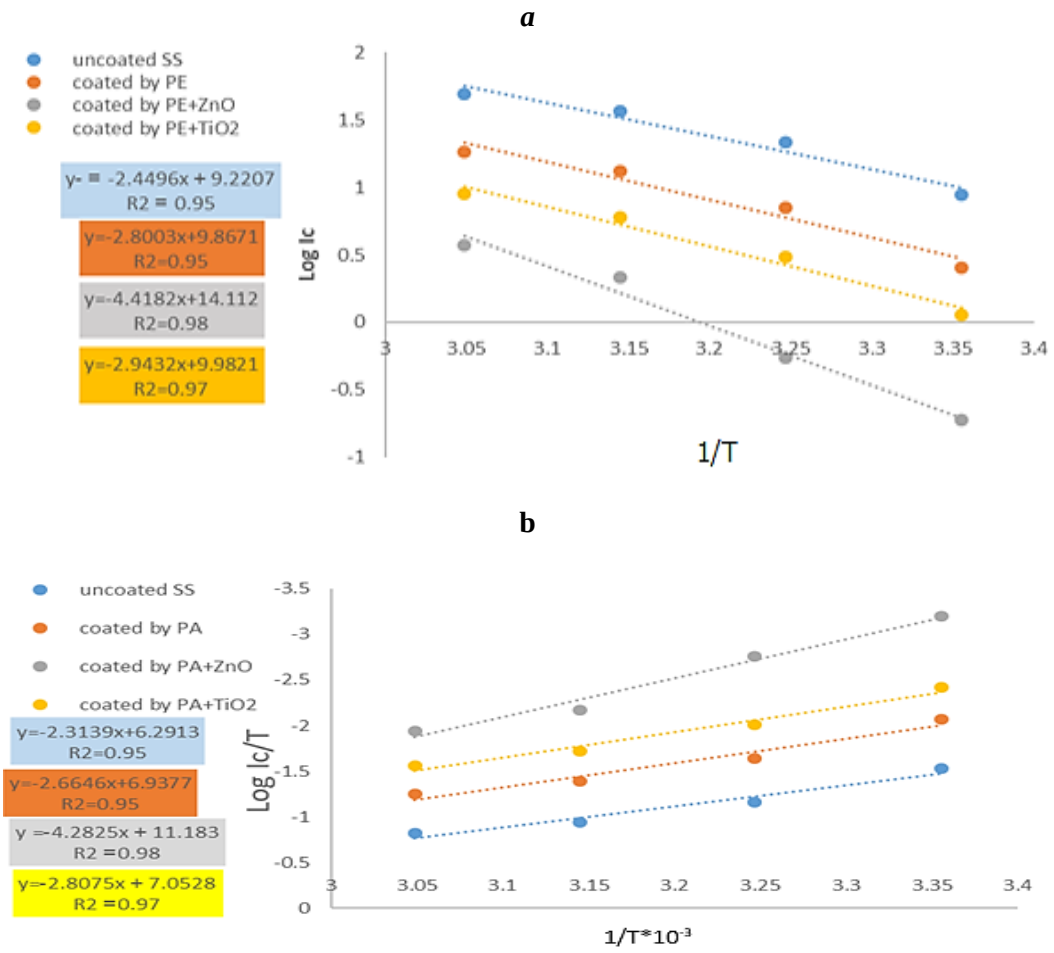

Figure 5. a-Plot of (log $Ic_{OR.}$) vs. (1/T) for SS- 304L before and after coating with PA and nano-PA b-Plot of (log $Ic_{OR.}$/T) vs (1/T) for SS -304L before and after coating with PA and nano-PA

Table 5. Transition state thermodynamic parameter at different temperatures for the corrosion of uncoated and coated SS-304L in 3.5% NaCl Solution.

	T(K)	ΔG (KJ)	ΔH (KJ/mol)	-ΔS (J/mol.K)	Ea (kJ/mol)	A (Molecule.Cm^{-2} .S^{-1})
Uncoated SS-304L (blank)	298	67.18	44.24	77.17	46.72	$9.99*10^{32}$
	308	67.95				
	318	68.72				
	328	69.49				
Coated SS-304L by PA	298	70.01	50.94	64.73	53.62	$4.36*10^{33}$
	308	70.65				
	318	71.29				
	328	71.93				
Coated SS-304L by (PA)+(n-ZnO)	298	100.61	81.96	62.68	84.64	$7.75*10^{37}$
	308	101.24				
	318	101.86				
	328	102.49				

2024, 21(4): 1243-1254
https://doi.org/10.21123/bsj.2023.8458
P-ISSN: 2078-8665 - E-ISSN: 2411-7986
Baghdad Science Journal

Coated SS-304L by (PA) +(n-TiO_2)		2982 298	72.40	53.81	62.57	56.3	$5.75*10^{33}$
		308	73.02				
		318	73.65				
		328	74.27				

The results generally demonstrated that the thermodynamic activation parameters (Ea and ΔH*) for the polymer-coated SS-304L are greater than those for the uncoated SS-304L. This suggests that the energy barrier has risen. Entropy of activation values for the polymer film-coated and uncoated SS-304L are negative, demonstrating that the activated complex in the rate-determining step was obtained in an association rather than a dissociation step and that there is less disordering when reactants are transferred to the activated complex[23].

Antimicrobial Activity of PA: The inhibitory zones of the polymers generated were evaluated on both bacteria species (*S. aureus and E. coli*) both when present and when absent of nanomaterials (ZnO, TiO_2) at a concentration of 800g/ml. Di - Methyl Sulfoxide was utilized as the solvent (DMSO). Table 6 summarizes the findings.

Table 6. (PA) inhibition zone both when present and when absent of the nanomaterial.

Samples	*(S. aureus)*(+Gram)	*(E. coli)*(-Gram)
PA	16	20
PA modified by ZnO	22	26
PA modified by TiO_2	18	30
Amoxicillin	30	30
DMSO	-	-

The polymer shown superior inhibitory effectiveness against both *S. aureus* and *E. coli* when compared to Amoxicillin. The polymer's capacity to kill bacteria is determined by it created a stable interaction complex by drug-bound topoisomerases and cleaved DNA. The polymer's suppression of topoisomerase activity and formation of stable complexes with DNA has a significant detrimental impact on cell[24]. Oxides-nanomaterials are becoming more significant in medical, pharmaceutical and biological uses as an antibacterial method in opposition to the spread of antibiotic-resistant bacteria and the resurgence of infectious illnesses[25] Nanoparticles are assumed to be biocidal effective because due to their tiny size and high surface-to-volume ratio, which enables them to come in touch with the membranes of microorganisms[25].

Discussion

From the FTIR tests in Fig. 3, it is noticed that the disappearance of the peak at the position of the $1680cm^{-1}$ after the electropolymerization process, was originally present in the monomer examination in Fig. 3a, evidence of the occurrence of the electropolymerization process. As for the AFM examination according to Fig. 4 and Table 3, the results indicate a decrease in the values of Rq, Ra and grain size after modification with nanomaterials.

Results in the Table 4 indicated that protection efficiency (PE%) is strongly influenced by temperature, with a fall in PE% values as temperature rising. This may be explained by the fact that as temperature increases, so did the thickness of the boundary layer[26]

Table 4. demonstrates that the WL and PL values are greatly dependent on temperature. Temperature has an effect on the WL and PL values, which increase as the temperature rising. All coating systems had the greatest WL and PL values at 328K. Also the values of WL and PL were lower in coated SS-304L than in uncoated SS-304L, and these values are clearly lower

2024, 21(4): 1243-1254
https://doi.org/10.21123/bsj.2023.8458
P-ISSN: 2078-8665 - E-ISSN: 2411-7986
Baghdad Science Journal

after adding nanomaterial. The porosity of the coating layer and the coating's capacity to inhibit entry of hostile anions such as chloride ion into the surface of SS-304L influenced these results[27]

Results in Table 5 indicated that the endothermic character of St.transition S.'s state reaction is shown by the positive activation enthalpies (ΔH*) for coated and uncoated SS-304L. Both the coated and uncoated SS-304L have negative values for ΔS*. Activation complexes in rate-determining steps indicate association rather than dissociation steps, according to this definition. Demonstrating that while moving from the reactant to the activated compound, disordering decreases[28,29] ·According to Table 5, the activation of free energy has a positive value. Moreover, almost minute variations were seen as the temperature rose, suggesting that the activated compounds were unstable and that rising temperatures lowered the likelihood of their production[30].

Furthermore, polymer film (PA) coated with nano material exhibits modest action against Gram negative bacteria *(E. coli)* and Gram positive bacteria *(B. subtilis) (S. aureus).*

Conclusion

SS-304L's PA and PA -composites coating was electropolymerized using a DC power supply technique in aqueous solution (3.5% NaCl). Potentiodynamic polarization was used to assess the polymer Nano composite coating's ability to prevent corrosion in a solution containing 3.5% NaCl. With rising temperatures, both the corrosion potential (Ecor) and corrosion current density (Icor) increased. After covering the SS-304L with polymer films in both the presence and absence of nanomaterials, the corrosion current density (icorr) decreased. Tafel plot indicated that the polymer film acts as anodic protection since the corrosion potential (Ecorr) of the SS-304L coated with the polymer film in the presence and absence of the Nano materials shifted to the noble direction in comparison to that of the uncoated SS-304L. Because they outperform bare SS-304L in terms of corrosion inhibition efficiency and protection efficiency (PE%), polymer Nano composite coatings exhibit excellent corrosion resistance. Additionally, due to their ease of preparation, reliable performance, and potent anti-corrosion properties, Nano composite materials have the potential to expand anti-corrosion applications. AFM analysis showed that the creation of protective coatings on the metal surface, which had stronger barrier effects, was what allowed SS-304L to be protected.

Authors' Declaration

- Conflicts of Interest: None.
- We hereby confirm that all the Figures and Tables in the manuscript are ours. Furthermore, any Figures and images, that are not ours, have been included with the necessary permission for re-publication, which is attached to the manuscript.
- Ethical Clearance: The project was approved by the local ethical committee in University of Baghdad.

Authors' Contribution Statement

Data was gathered, examined, and outcomes were interpreted by A. M. N. The research plan was created, results were tracked, and the manuscript was proofread by K. A. S.

References

1. Rajasekharan V, Stalin T, Viswanathan S, Manisankar P. Electrochemical evaluation of anticorrosive performance of organic acid doped polyaniline based coatings. Int J Electrochem Sci. 2013 Sep 1; 8: 11327-36.. https://doi.org/10.1016/j.jcis.2023.01.097
2. Laska-Lesniewicz A, Szczepanska P, Kaminska M, Nowosielska M, Sobczyk-Guzenda A. 6-step

manufacturing process of hydroxyapatite filler with specific properties applied for bone cement composites. Ceram Int. 2022 Sep 15; 48(18): 26854-64.https://doi.org/10.1016/j.ceramint.2022.05.387

3. Saleh WR, Ali AM, Hassan TA, Assi AA, Hassan SM. Fabrication of PANI by electropolymerization method on SnO2 conductive glass as counter electrode for dye sensitive solar cell. Int J Curr Eng Technol. 2014; 4 (6): 4004-4010 : https://www.researchgate.net/publication/269092960
4. Altıncı OC, Körbahti BK. Graphene oxide-polyaniline conducting composite film deposited on platinum-iridium electrode by electrochemical polymerization of aniline: Synthesis and environmental electrochemistry application. Appl Surf Sci.. 2022 Feb 1; 7: 100212. https://doi.org/10.1016/j.apsadv.2022.100212
5. Yağan A. Corrosion performances of polyaniline and poly (N-methylaniline) coated stainless steel by impedance spectroscopy. Int J Electrochem Sci. 2019 Mar 1; 14: 2906-13. doi: 10.20964/2019.03.77
6. Abdulmajeed MH, Abdullah HA, Ibrahim SI, Alsandooq GZ. Investigation of corrosion protection for steel by eco-friendly coating. .. J Eng Technol. 2019 Feb 25; 37(2): 52-9. https://doi.org/10.30684/etj.37.2A.3
7. Hosseinzade MR, Naji L, Hasannezhad F. Electrochemical deposition of NiO bunsenite nanostructures with different morphologies as the hole transport layer in polymer solar cells J Electroanal Chem. 2022 Dec 1; 926: 116955.
8. Kubo I, Fujita KI, Nihei KI. Antimicrobial activity of anethole and related compounds from aniseed. J Sci Food Agric. 2008 Jan 30; 88(2): 242-7. https://doi.org/10.1002/jsfa.3079
9. Soares PM, Lima RF, de Freitas Pires A, Souza EP, Assreuy AM, Criddle DN. Effects of anethole and structural analogues on the contractility of rat isolated aorta: Involvement of voltage-dependent Ca2+-channels. Life Sci. 2007 Sep 8; 81(13): 1085-93. https://doi.org/10.1016/j.lfs.2007.08.027
10. Aprotosoaie AC, Costache II, Miron A. Anethole and its role in chronic diseases. Adv Exp Med Biol. 2016; 929: :247-67. https://doi.org/10.1007/978-3-319-41342-6_11
11. Cerrai P, Guerra G, Tricoli M, Nucci L. Electro-initiated cationic polymerizations-VI: Anodic electrochemical behaviour and direct electropolymerization of anethole in 1, 2-dichloroethane. Eur Polym J. 1980 Jan 1; 16(9): 867-73. https://doi.org/10.1016/0014-3057(80)90118-4
12. Hulnik MI, Kuharenko OV, Vasilenko IV, Timashev P, Kostjuk SV. Quasiliving Cationic Polymerization of Anethole: Accessing High-Performance Plastic from the Biomass-Derived Monomer. ACS Sustainable Chem Eng. 2021 May 3; 9(19): 6841-54. https://doi.org/10.1021/acssuschemeng.1c01504
13. Yakovenko OS, Matzui LY, Vovchenko LL, Trukhanov AV, Kazakevich IS, Trukhanov SV, et al. Magnetic anisotropy of the graphite nanoplatelet–epoxy and MWCNT–epoxy composites with aligned barium ferrite filler. J Mater Sci. 2017 May; 52: 5345-58. https://doi.org/10.1007/s10853-017-0776-4
14. Contri G, Barra GM, Ramoa SD, Merlini C, Ecco LG, Souza FS, Spinelli A. Epoxy coating based on montmorillonite-polypyrrole: Electrical properties and prospective application on corrosion protection of steel Prog Org Coat. 2018 Jan 1; 114: 201-7. https://doi.org/10.1016/j.porgcoat.2017.10.008
15. Mohammed R, Saleh K. A novel conducting polyamic acid/nanocomposite coating for corrosion protection. . Eurasian Chem Commun. 2021; 3: 715-25. https://doi.org/10.22034/ecc.2021.296065.1206
16. Al-Mashhadani HA, Saleh KA. Electro-polymerization of poly Eugenol on Ti and Ti alloy dental implant treatment by micro arc oxidation using as Anti-corrosion and Anti-microbial. Res J Pharm Technol. 2020; 13(10): 4687-96. https://doi.org/10.5958/0974-360X.2020.00825.2
17. Kubba RM, Mohammed MA, Ahamed LS. DFT Calculations and Experimental Study to Inhibit Carbon Steel Corrosion in Saline Solution by Quinoline-2-One Derivative. Baghdad Sci J. 2021; 18(1): 113-123. https://doi.org/10.21123/bsj.2021.18.1.0113
18. Molaei M, Fattah-alhosseini A, Nouri M, Mahmoodi P, Navard SH, Nourian A. Enhancing cytocompatibility, antibacterial activity and corrosion resistance of PEO coatings on titanium using incorporated ZrO2 nanoparticles. Surf Interfaces. 2022 Jun 1; 30: 101967. https://doi.org/10.1016/j.surfin.2022.101967
19. Li Z. et al ,Rhamnolipid as an eco-friendly corrosion inhibitor for microbiologically influenced corrosion. Corros Sci. 2022 Aug 1; 204: 110390. https://doi.org/10.1016/j.corsci.2022.110390
20. Mohammed MA, Kubba RM. Experimental Evaluation for the Inhibition of Carbon Steel Corrosion in Salt and Acid Media by New Derivative of Quinolin-2-One. Iraqi J Sci. 28;61(8) :1861-73. https://doi.org/10.24996/ijs.2020.61.8.2
21. Talbot DE, Talbot JD. Corrosion science and technology. CRC press, Third Edition,; 2018 Jan 29: 195-199.https://doi.org/10.1201/9781351259910
22. Farag ZR, Moustapha ME, Abd El-Hafeez GM. The inhibition tendencies of novel hydrazide derivatives on the corrosion behavior of mild steel in

2024, 21(4): 1243-1254
https://doi.org/10.21123/bsj.2023.8458
P-ISSN: 2078-8665 - E-ISSN: 2411-7986
Baghdad Science Journal

hydrochloric acid solution. J Mater Res Technol. 2022 Jan 1; 16: 1422-34 https://doi.org/10.1016/j.jmrt.2021.12.035
23. Jassim RA, Farhan AM, Ali AM. Corrosion protection study of carbon steel and 316 stainless steel alloys coated by nanoparticles. Baghdad Sci J. 2014; 11(1): 116-122. https://doi.org/10.21123/bsj.2014.11.1.116-122
24. Jiang Y, Zheng W, Tran K, Kamilar E, Bariwal J, Ma H, et al . Hydrophilic nanoparticles that kill bacteria while sparing mammalian cells reveal the antibiotic role of nanostructures. Nat Commun. 2022 Jan 11;13(1):197.. Nat Commun. 2022; 197(13) : 1-17. https://doi.org/10.1038/s41467-021-27193-9
25. Almashhadani HA, Alshujery MK, Khalil M, Kadhem MM, Khadom AA. Corrosion inhibition behavior of expired diclofenac Sodium drug for Al 6061 alloy in aqueous media: Electrochemical, morphological, and theoretical investigations. J Mol Liq. 2021 Dec 1; 343: 117656. https://doi.org/10.1016/j.molliq.2021.117656.
26. Wang Y, Chen T, Wang H, Hu J, Ma Y, Wei J, et al .Corrosion inhibition effect of zeolitic imidazolate framework in chloride-contaminated cement pore solution under elevated temperatures. Constr Build Mater. 2022 Aug 1; 342: 128024. https://doi.org/10.1016/j.conbuildmat.2022.128024
27. Abu Hassan Shaari H, Ramli MM, Mohtar MN, Abdul Rahman N, Ahmad A. Synthesis and conductivity studies of poly (Methyl Methacrylate)(PMMA) by co-polymerization and blending with polyaniline (PANi ,Polymers . 2021 Jun 11; 13(12): 1939. https://doi.org/10.3390/polym13121939
28. Mohammed IM. Experimental and Quantum Chemical Studies on the Corrosion Inhibition of Mild Steel By 2-((Thiophen-2-Ylmethylene) Amino) Benzenethio in 1M HCl. Baghdad Sci J. 2019; 16(1): 49-55. https://doi.org/10.21123/bsj.2019.16.1.0049
29. Abdulridha AA, Allah MA, Makki SQ, Sert Y, Salman HE, Balakit AA. Corrosion inhibition of carbon steel in 1 M H2SO4 using new Azo Schiff compound: electrochemical, gravimetric, adsorption, surface and DFT studies. .. J Mol Liq. 2020 Oct 1; 315: 113690. https://doi.org/10.1016/j.molliq.2020.113690
30. Saleh KA, Ali MI. Electro polymerization for (N-Terminal tetrahydrophthalamic acid) for Anti-corrosion and Biological Activity Applications.. Iraqi J Sci.. 2020; 61(1): 1-12.

تخليق بوليمرات موصلة كهربائياً من البولي أثينول / أكاسيد المعادن النانوية للحماية من التأكل والنشاط البكتيري

ايات منذر نعمان ، خلود عبد صالح

قسم الكيمياء، كلية العلوم، جامعة بغداد، بغداد، العراق.

الخلاصة

للتأكل اهمية كبيرة للباحث بسبب تأثيره الكبير على سلامة الناس واقتصادهم بشكل مباشر. ولحماية معدن الفولاذ المقاوم للصدأ نوع 304L بأستخدام عملية البلمرة الكهربائية لتخليق بوليمرات موصلة ومن ثم تحسينها بـأستخدام مواد نانوية.تم تخليق بوليمر الانيثول كهربائيا على شكل طبقة طلاء لسبائك الفولاذ المقاوم للصدأ ومن ثم اجراء الفحوصات المختبرية من التشخيص بتقنية الاشعة تحت الحمراء ومطيافية القوة الذرية للبوليمر المحضر لوحده مرة ومع الاكاسيد النانوية مرة اخرى.النتائج بينت تقليل كثافة تيار التأكل بعد تخليق الطلاء على السبيكة مما لو كانت السبيكة لوحدها وان نسبة الحماية قد ارتفعت من 71% للبولي انيثول الى 87% بأستخدام TiO_2 والى 98% بأستخدام ZnO. كذلك تم حساب الدوال او المعاملات الحركية والثرموديناميكية (Ea, A, ΔH, ΔS, ΔG) لعملية التأكل.تضمن البحث دراسة الفعالية البايولوجية للبوليمر المحضر ضد سلالات البكتريا وهي المكورات العنقودية الذهبية والاشريكية القولونية بوجود وعدم وجود المواد النانوية لزيادة كفاءة الطبقة البوليمرية ضد التأكل والبكتريا.

الكلمات المفتاحية: أنيثول, التأكل , بلمرة كهربائية ,مركبات نانوية, بولي أنيثول.